

Preparation of surfactant-stabilized gold nanoparticle–peptide nucleic acid conjugates

Janice Duy · Laurie B. Connell · Wolfgang Eck ·
Scott D. Collins · Rosemary L. Smith

Received: 26 February 2010 / Accepted: 7 June 2010 / Published online: 20 June 2010
© Springer Science+Business Media B.V. 2010

Abstract A simple, two-step method of producing stable and functional peptide nucleic acid (PNA)-conjugated gold nanoparticles using a surfactant stabilization step is presented. PNA are DNA analogs with superior chemical stability and target discrimination, but their use in metallic nanoparticle systems has been limited by the difficulty of producing stable colloids of nanoparticle–PNA conjugates. In this work, the nonionic surfactant Tween 20 (polyoxyethylene (20) sorbitan monolaurate) was used to sterically shield gold surfaces prior to the addition of thiolated PNA, producing conjugates which remain dispersed in solution and retain the ability to hybridize to

complementary nucleic acid sequences. The conjugates were characterized using transmission electron microscopy, dynamic light scattering, and UV–visible absorbance spectroscopy. PNA attachment to gold nanoparticles was confirmed with an enzyme-linked immunoassay, while the ability of nanoparticle-bound PNA to hybridize to its complement was demonstrated using labeled DNA.

Keywords Gold nanoparticles · Peptide nucleic acid · Tween 20 · PNA–DNA hybridization

Introduction

DNA–gold nanoparticle conjugates belong to a class of hybrid materials that merge the specific molecular recognition ability of biomaterials with the size-tunable chemical and physical properties of nanoscale materials. They have a wide range of applications including biosensing, targeted drug delivery and gene regulation (Rosi and Mirkin 2005). The conjugation of DNA to gold nanoparticles was first reported in 1996 for the formation of larger particle assemblies organized by sequence-specific DNA hybridization (Alivisatos et al. 1996; Mirkin et al. 1996). The attachment of DNA to gold nanoparticles is uncomplicated since thiol-terminated DNA strands attach strongly and specifically to gold surfaces, and the negatively charged phosphate backbones of the strands maintain electrostatic repulsion between

J. Duy (✉)
Graduate School of Biomedical Sciences, University
of Maine, Orono, ME, USA
e-mail: janice.duy@umit.maine.edu

L. B. Connell
School of Marine Sciences, University of Maine, Orono,
ME, USA

W. Eck
Applied Physical Chemistry, University of Heidelberg,
Heidelberg, Germany

S. D. Collins
Department of Chemistry, University of Maine, Orono,
ME, USA

R. L. Smith
Electrical and Computer Engineering Department,
University of Maine, Orono, ME, USA

individual gold nanoparticles (Mirkin et al. 1996). Stable gold nanoparticle–DNA conjugate dispersions (where the particles do not aggregate uncontrollably) can thus be produced while maintaining the ability of DNA to hybridize to complementary strands.

However, the limited chemical stability of DNA (Lindahl 1993) compromises its utility in “dirty” field environments or in complex sample matrices. Peptide nucleic acid (PNA), a DNA mimic, has gained recent attention as a superior probe molecule for such applications. PNA consists of an uncharged polyamide backbone made of repeating *N*-(2-aminoethyl)glycine units; nucleobases are joined to the backbone by methylene carbonyl linkages (Nielsen et al. 1991). PNA hybridizes to complementary DNA and RNA sequences due to comparable intermolecular distances and nucleobase configurations (Nielsen et al. 1991; Egholm et al. 1992; Egholm et al. 1993), while its uncharged peptide backbone creates a more discriminating probe molecule. Its lack of electrostatic repulsion to DNA strands allows PNA to bind complementary sequences even in solutions of low ionic strength, and while PNA–DNA duplexes exhibit a higher thermal stability than corresponding DNA–DNA duplexes, sequence mismatches are more destabilizing (Egholm et al. 1993). In addition, PNA is chemically robust and is not susceptible to degradation by nucleases or proteases (Demidov et al. 1994).

Despite these advantages of PNA, it has not superseded DNA in nanoparticle-based schemes because the attachment of PNA to gold nanoparticles has so far proven difficult (Lytton-Jean et al. 2009; Murphy et al. 2004). The addition of thiolated PNA to citrate-stabilized gold nanoparticle dispersions results in the immediate agglomeration and precipitation of the particles. The uncharged, thiolated PNA strands presumably displace citrate anions from the gold surface, allowing these uncovered areas to bind irreversibly to other exposed gold cores, making the dispersions highly unstable. To date, reports of successful attachment of PNA to gold nanoparticles have required the use of unconventional probe motifs. Negative charges were imparted to PNA strands either from amino acid residues at the tethered end (Chakrabarti and Klibanov 2003; Murphy et al. 2004), or through the creation of PNA–DNA chimeras (Murphy et al. 2004). Although these modifications have allowed for the conjugation of PNA to gold nanoparticles without loss of colloid stability, PNA functionality was compromised.

In this work, a facile method for producing stable and functional gold nanoparticle–PNA (AuNP–PNA) conjugates is presented. The nonionic surfactant polyoxyethylene (20) sorbitan monolaurate (Tween 20) was used to mediate the exchange between the citrate anions on the surface of the gold nanoparticles and thiolated PNA strands. Surfactant concentrations above the critical micelle concentration (CMC) have previously been shown to prevent the aggregation of gold nanoparticles through the physisorption of free surfactant molecules prior to the chemisorption of alkanethiols (Aslan and Perez-Luna 2002). Similarly in this work, Tween 20 was added in large excess and allowed to adsorb onto the gold nanoparticle surfaces prior to the addition of thiolated PNA. Excess surfactant and PNA were removed by centrifugation and rinsing with dilute surfactant solution. The AuNP–PNA conjugates were then resuspended in fresh dilute surfactant solution to maintain the steric protection provided by the surfactant molecules. Characterization of the particle size distributions of citrate-stabilized, surfactant-stabilized, and PNA-conjugated gold dispersions was performed using transmission electron microscopy (TEM), dynamic light scattering (DLS), and UV–visible absorbance spectroscopy. PNA attachment onto gold nanoparticles and the hybridization of gold nanoparticle-bound PNA to complementary labeled DNA sequences were verified using enzyme-linked immunoassays.

Materials and methods

Chemicals and reagents

Gold(III) chloride trihydrate, trisodium citrate dihydrate, sodium chloride, Tween 20, and sulfuric acid were purchased from Sigma-Aldrich (USA). Horseradish peroxidase-conjugated streptavidin, peroxidase-conjugated anti-digoxin, and 3,3',5,5'-tetramethylbenzidine (TMB) were purchased from Pierce (USA). Milli-Q water with resistance >18 M Ω /cm was used in all the experiments.

Oligonucleotides

All oligonucleotide sequences used are shown in Table 1. PNA sequences were purchased from

Table 1 Oligonucleotide sequences used in this study

Name	Sequence (N–C/5'–3')
PNA UniR	N-HS-OOOO-CAGCMGCCGCGGTAATWC-EE-Biotin-C
PNA 008	N-Biotin-EE- <i>GTGCAACAATCCACC</i> -OOOO-SH-C
PNA 010	N-Biotin-EE- CAACACCATGTGAACTG -OOOO-SH-C
DNA linker	5'- <i>GGTGGGATTGTGCAC</i> -TTTTTTT-Digoxigenin-TTTTTT- CAGTTCACATGGTGTG -3'

Italicized portions of the DNA linker are complementary to PNA 008, while portions in bold are complementary to PNA 010. E linkers in the PNA sequences were added to prevent self-aggregation, while O spacers extend the immobilized probe sequence from the surface. The UniR sequence contains the degenerate bases M (either adenosine or cytosine) and W (either adenosine or thymine)

Panagene (Korea). The DNA linker sequence was obtained from Integrated DNA Technologies (USA).

Gold nanoparticle synthesis and characterization

Gold nanoparticles were synthesized by the reduction of 1 mM gold(III) chloride trihydrate with 30 mM trisodium citrate dihydrate (Grabar et al. 1995). The resulting particles were characterized using TEM, DLS, and UV–visible absorbance spectroscopy. A Philips CM-10 transmission electron microscope (accelerating voltage 92 kV) equipped with a Gatan BioScan model 792 digital camera was used to image gold nanoparticles. DLS measurements were performed at 20 °C using a Zetasizer Nano ZS (Malvern Instruments, UK) with a 4 mW He–Ne laser (633 nm wavelength), and the solvent refractive index was set to 1.330, while the complex index of refraction of the particles was set to $n = 0.2$ and $k = 3.32$. Absorbance spectroscopy was performed using a NanoVue spectrophotometer (GE Healthcare) using a 4 μ L sample solution volume.

Preparation of AuNP–PNA conjugates

Solutions of 10% (v/v) Tween 20 in water (final concentration 84.6 mg/mL) and citrate-stabilized gold nanoparticles (final concentration 3.97 nM) were mixed and allowed to react for 30 min in a rotisserie-type shaker at room temperature. Next, 860 pmol of biotin-labeled, thiol-terminated PNA (final concentration 132.3 nM) was added and incubated at room temperature in a shaker for 24 h. The resulting dispersion was rinsed twice by centrifugation at 15,700g for 15 min and then resuspended in a solution of 0.02% (v/v) Tween 20 in water.

Enzymatic assessment of PNA attachment to AuNPs

PNA attachment to gold nanoparticles was confirmed using the free biotin label at the end of each PNA sequence. Gold nanoparticle dispersions were standardized to 25% of the original (citrate-stabilized) concentration at 506 nm (Liu et al. 2007). Horseradish peroxidase-conjugated streptavidin SA-HRP, 990 μ L of 300 ng/mL concentration in 0.02% Tween 20, was added to 10 μ L of diluted gold nanoparticle dispersion and allowed to react for 30 min in a shaker at room temperature. Excess SA-HRP was removed through five rinses by centrifugation with 0.02% Tween 20 in water. The resulting pellet from the last centrifugation was mixed with 100 μ L TMB and incubated for 5 min. The formation of a blue product from the reaction of TMB in the presence of horseradish peroxidase was measured at 370 and 650 nm, the major absorbance peaks of oxidized TMB.

Verification of functionality and specificity of AuNP–PNA conjugates

Digoxigenin-labeled DNA (10 pmol, 10 nM final concentration) in a solution of 200 mM sodium phosphate dibasic, pH 8.1 with 0.02% Tween 20, was added to 6.48 nM of gold nanoparticle dispersion and allowed to hybridize for 30 min at room temperature. The excess DNA was removed by five rinses by centrifugation with BSA blocker (bovine serum albumin 0.5% (w/v), Tween 20 0.05% (v/v) in phosphate-buffered saline pH 7.4) to prevent nonspecific antibody adsorption in the next step. The remaining pellet was reacted with 1:1000 (v/v) horseradish peroxidase-conjugated anti-digoxin (anti-dig HRP) in BSA blocker for 30 min at

room temperature. Excess anti-dig HRP was removed by rinsing and centrifugation as described above. The pellet was mixed with TMB, and solution absorbance peaks were read at 370 and 650 nm.

Results and discussion

Characterization of gold nanoparticle dispersions

TEM images (Fig. 1) of the effect of surfactant adsorption onto gold nanoparticles before and after the addition of thiolated PNA are shown in contrast to citrate-stabilized particles. Figure 1a and b, respectively, show surfactant- and citrate-stabilized particles before the addition of thiolated PNA. The surfactant-stabilized particles remain dispersed, with minimal aggregation, after PNA attachment (Fig. 1c), while the citrate-stabilized particles formed large crosslinked aggregates (Fig. 1d). The AuNP–PNA conjugates were also stable in buffers containing up to 0.3 M NaCl for several months (data not shown). Mean diameters obtained from the TEM images were 14.26 ± 2.46 nm (citrate-stabilized particles), $16.25 \pm$

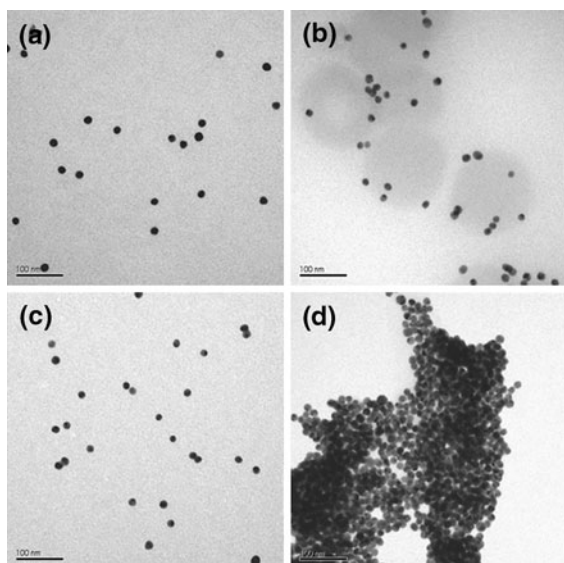


Fig. 1 TEM images of gold nanoparticle dispersions. Surfactant-stabilized dispersions **a** before and **b** after the addition of thiolated PNA. Citrate-stabilized dispersions **c** before and **d** after the addition of thiolated PNA. The scale bar in each image is 100 nm

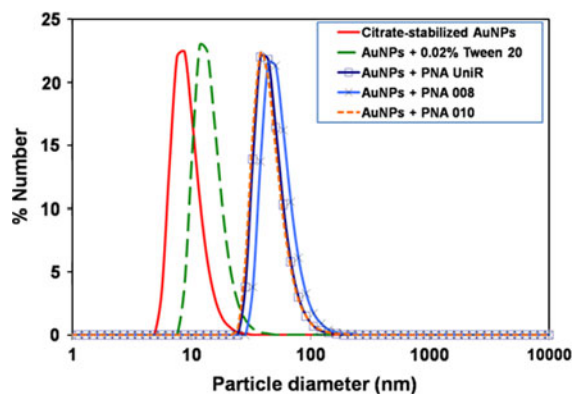


Fig. 2 Particle size distributions by number of gold nanoparticle solutions show increased particle sizes in the samples exposed to thiolated PNA, indicating the formation of PNA-conjugated gold nanoparticles

1.14 nm (surfactant-modified), and 16.05 ± 1.62 nm (PNA-modified).

The particle size distributions of the gold nanoparticle systems obtained by DLS were monomodal, with narrow peaks (Fig. 2), indicating disperse particles. The citrate-stabilized particles yielded a DLS-determined mean diameter (Z-average diameter) of 24.09 nm, while the surfactant-modified particles yielded a somewhat larger mean diameter of 29.67 nm without the formation of any additional peaks. The AuNP–PNA conjugates yielded much larger mean diameters of 98.10, 93.42, and 102 nm for PNA UniR, PNA 008, and PNA 010, respectively. Since the analysis of TEM images of gold nanoparticles before and after the surfactant-mediated attachment of PNA revealed no apparent differences in particle diameters, and no fused gold cores, this discrepancy in diameter enlargement could be due to the formation of small aggregates in solution, possibly due to the weak adsorption of the biotin label (which contains a sulfide group) to gold surfaces (Love et al. 2005). In contrast, DLS particle size distributions of gold nanoparticle dispersions functionalized with the same PNA sequences but labeled with a Cy5 fluorophore yielded a Z-average diameter of 36 nm.

Normalized optical absorption spectra for the gold nanoparticle dispersions are shown in Fig. 3. The absorbance peak of the unmodified particles was at ~ 520 nm, while that of the surfactant-stabilized particles was shifted to 523 nm. The absorbance peak of the AuNP–PNA conjugates was further shifted to

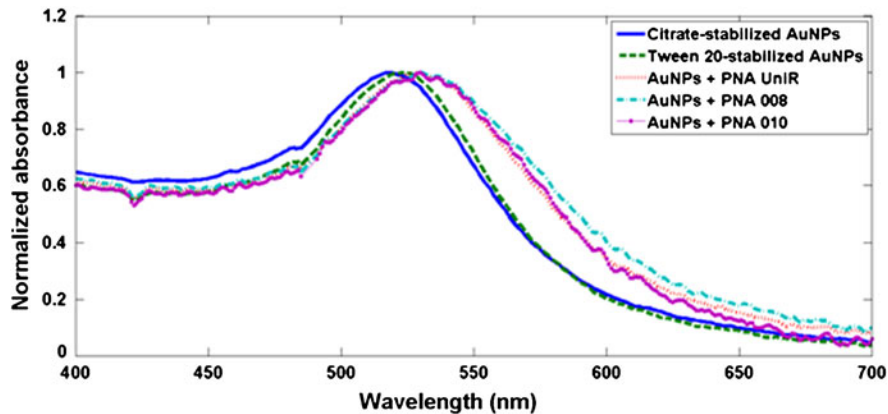


Fig. 3 Absorbance spectra of gold nanoparticle dispersions. The surfactant- and PNA-treated particles exhibit slight shifts in absorbance peak wavelengths, due to the alteration of the dielectric constant immediately surrounding the particles.

~530 nm, with a slight increase in the absorbance values at longer wavelengths (>600 nm). These shifts are consistent with previously reported results for surfactant- (Aslan and Perez-Luna 2002) and DNA-coated (Xu and Craig 2005) gold nanoparticles. These observed absorbance shifts are most likely due to changes in the dielectric properties of the layer immediately surrounding the gold nanoparticles (Mulvaney 1996; Schmitt et al. 1999; Eck et al. 2001), and to some small amount of particle aggregation. Again, biotin-gold interactions could be responsible for this effect, as absorbance spectra obtained from gold nanoparticles functionalized with Cy5-labeled PNA only exhibited a 2-nm peak shift, without absorbance increases at longer wavelengths.

Verification of PNA attachment to gold nanoparticles

The addition of TMB to AuNP–PNA conjugate dispersions treated with SA-HRP resulted in large increases in absorbance at both 370 and 650 nm compared to both citrate-stabilized and Tween 20-treated gold nanoparticles (Fig. 4), indicative of the oxidation of TMB and hence the presence of attached PNA. The changes in peak absorbance values differed for the three PNA sequences tested, with increases of 12, 10, and 5 times that of the Tween 20-stabilized particles for the PNA UniR, PNA 008, and PNA 010, respectively.

Nanoparticles with PNA also show increases in absorbance values at longer (>600 nm) wavelengths, possibly due to interactions between the gold surface and biotinylated PNA ends which lead to a small amount of aggregation

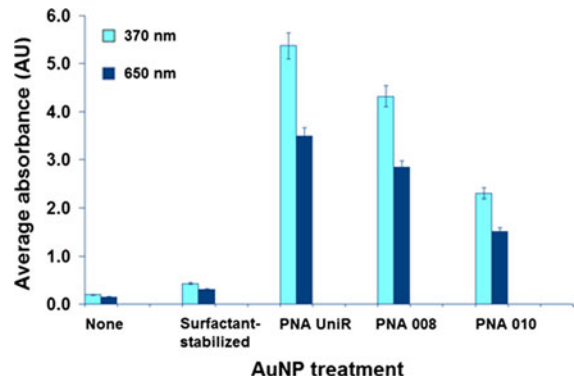


Fig. 4 Verification of biotinylated PNA attachment to gold nanoparticles through the oxidation of tetramethylbenzidine (TMB) by horseradish peroxidase-conjugated streptavidin (SA-HRP). SA-HRP was allowed to bind to biotinylated PNA and unreacted molecules were removed by washing before the addition of TMB, which is oxidized by horseradish peroxidase. TMB develops absorbance peaks at 370 and 650 nm when it is oxidized

Specific hybridization of AuNP–PNA conjugates to complementary DNA

Increases in TMB absorbance peak values due to the specific hybridization of PNA probe-coated gold nanoparticles are shown in Fig. 5. Background levels of absorbance at 370 and 650 nm were observed for gold nanoparticle dispersions without complementary DNA, and for unmodified and negative control PNA UniR-coated nanoparticles with target DNA. AuNP–PNA conjugates allowed to hybridize with

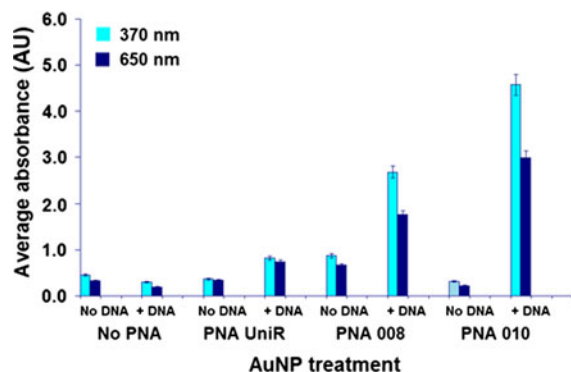


Fig. 5 Hybridization of complementary digoxigenin-labeled DNA to AuNP–PNA conjugates verified using the oxidation of tetramethylbenzidine (TMB) by horseradish peroxidase-conjugated anti-digoxin (anti-dig HRP). The development of TMB absorbance peaks at 370 nm and 650 nm indicate DNA hybridization

complementary DNA exhibited greater than a 2.5-fold increase in absorbance at 370 nm over the background level. Observed differences in the amount of hybridized DNA target to PNA 008 and PNA 010 could be ascribed to sequence-dependent PNA characteristics, which may have affected particle surface coverage (Demers et al. 2000) and hybridization kinetics (Kushon et al. 2001; Peterson et al. 2001; Armitage 2003). The presence of free surfactant molecules in solution should not have affected DNA recognition, since detergents in concentrations of up to 0.1% are routinely used in hybridization buffers for PNA hybridization (Williams et al. 2002).

Conclusions

In this work, stable and functional gold nanoparticle–PNA (AuNP–PNA) conjugates created using an intermediate surfactant stabilization step are described for the first time. The conjugation procedure is uncomplicated and requires no special modifications to commercially available thiolated PNA sequences. The resulting conjugates retain both the spectral characteristics of gold nanoparticles and the ability of PNA to hybridize to its complement. This hybrid nanomaterial can now be exploited in nanoparticle-based DNA sensing applications where the charge neutrality, chemical robustness and high target discrimination of PNA improves performance.

Acknowledgments The authors would like to thank Dr. Michael D. Mason and Dr. Paul Millard for sharing their resources and expertise. Support for this work has been generously provided by the Functional Genomics National Science Foundation-Integrative Graduate Education and Research Traineeship (NSF-IGERT) grant #0221625, National Oceanic and Atmospheric Administration (NOAA) Center for Sponsored Coastal Ocean Research (CSCOR) Monitoring and Event Response for Harmful Algal Blooms (MERHAB) program NA05NOS4781232, and the United States Department of Agriculture (USDA) Biosecurity award #2006-55605-16654.

References

- Alivisatos AP, Johnsson KP, Peng X, Wilson TE, Loweth CJ, Bruchez MPI, Schultz PG (1996) Organization of ‘nanocrystal molecules’ using DNA. *Nature* 382:609–611
- Armitage BA (2003) The impact of nucleic acid secondary structure on PNA hybridization. *Drug Discovery Today* 8:222–228
- Aslan K, Perez-Luna VH (2002) Surface modification of colloidal gold by chemisorption of alkanethiols in the presence of a nonionic surfactant. *Langmuir* 18:6059–6065
- Chakrabarti R, Klibanov AM (2003) Nanocrystals modified with peptide nucleic acids (PNAs) for selective self-assembly and DNA detection. *J Am Chem Soc* 125:12531–12540
- Demers LM, Mirkin CA, Mucic RC, Reynolds RA, Letsinger RL, Elghanian R, Viswanadham G (2000) A fluorescence-based method for determining the surface coverage and hybridization efficiency of thiol-capped oligonucleotides bound to gold thin films and nanoparticles. *Anal Chem* 72:5535–5541
- Demidov VV, Potaman VN, Frank-Kamenetskii MD, Egholm M, Buchardt O, Sonnichsen SH, Nielsen PE (1994) Stability of peptide nucleic acids in human serum and cellular extracts. *Biochem Pharmacol* 48:1310–1313
- Eck D, Helm CA, Wagner NJ, Vaynberg KA (2001) Plasmon resonance measurements of the adsorption and adsorption kinetics of a biopolymer onto gold nanocolloids. *Langmuir* 17:957–960
- Egholm M, Buchardt O, Nielsen PE, Berg RH (1992) Peptide nucleic acids (PNA). Oligonucleotide analogues with an achiral peptide backbone. *J Am Chem Soc* 114:1895–1897
- Egholm M, Buchardt O, Christensen L, Behrens C, Freier SM, Driver DA, Berg RH, Kim SK, Norden B, Nielsen PE (1993) PNA hybridizes to complementary oligonucleotides obeying the Watson-Crick hydrogen-bonding rules. *Nature* 365:566–568
- Grabar KC, Freeman RG, Hommer MB, Natan MJ (1995) Preparation and characterization of Au colloid layers. *Anal Chem* 67:735–743
- Kushon SA, Jordan JP, Seifert JL, Nielsen H, Nielsen PE, Armitage BA (2001) Effect of secondary structure on the thermodynamics and kinetics of PNA hybridization to DNA hairpins. *J Am Chem Soc* 123:10805–10813

- Lindahl T (1993) Instability and decay of the primary structure of DNA. *Nature* 362:709–715
- Liu X, Atwater M, Wang J, Huo Q (2007) Extinction coefficient of gold nanoparticles with different sizes and different capping ligands. *Colloids Surf B* 58:3–7
- Love JC, Estroff LA, Kreibel JK, Nuzzo RG, Whitesides GM (2005) Self-assembled monolayers of thiolates on metals as a form of nanotechnology. *Chem Rev* 105:1103–1169
- Lytton-Jean AKR, Gibbs-Davis JM, Long H, Schatz GC, Mirkin CA, Nguyen ST (2009) Highly cooperative behavior of peptide nucleic acid-linked DNA-modified gold-nanoparticle and comb-polymer aggregates. *Adv Mater* 21:706–709
- Mirkin CA, Letsinger RL, Mucic RC, Storhoff JJ (1996) A DNA-based method for rationally assembling nanoparticles into macroscopic materials. *Nature* 382:607–609
- Mulvaney P (1996) Surface plasmon spectroscopy of nanosized metal particles. *Langmuir* 12:788–800
- Murphy D, Redmond G, de la Torre BG, Eritja R (2004) Hybridization and melting behavior of peptide nucleic acid (PNA) oligonucleotide chimeras conjugated to gold nanoparticles. *Helv Chim Acta* 87:2727–2734
- Nielsen PE, Egholm M, Berg RH, Buchardt O (1991) Sequence-selective recognition of DNA by strand displacement with a thymine-substituted polyamide. *Science* 254:1497–1500
- Peterson AW, Heaton RJ, Georgiadis RM (2001) The effect of surface probe density on DNA hybridization. *Nucleic Acids Res* 29:5163–5168
- Rosi NL, Mirkin CA (2005) Nanostructures in biodiagnostics. *Chem Rev* 105:1547–1562
- Schmitt J, Machtle P, Eck D, Mohwald H, Helm CA (1999) Preparation and optical properties of colloidal gold monolayers. *Langmuir* 15:3256–3266
- Williams B, Stender H, Coull JM (2002) PNA fluorescent in situ hybridization for rapid microbiology and cytogenetic analysis. In: Nielsen PE (ed) *Methods in molecular biology*. Humana Press Inc., Totowa, pp 181–194
- Xu J, Craig SL (2005) Thermodynamics of DNA hybridization on gold nanoparticles. *J Am Chem Soc* 127:13227–13231